

Numerical Solution of the Discharge Coefficient of Trapezoidal Arced Labyrinth Weirs with Different Middle Cycles Using Flow 3D Software

Jamal Feili¹, Mohammad Heidarnejad^{2*}, Alireza Masjedi³, Mahdi AsadiLor⁴


1- PhD Student, Department of Water Science Engineering, Ahvaz Branch, Islamic Azad University, Ahvaz, Iran.

2- Associate Professor, Department of Water Science Engineering, Ahvaz Branch, Islamic Azad University, Ahvaz, Iran.

3- Professor, Department of Water Science Engineering, Ahvaz Branch, Islamic Azad University, Ahvaz, Iran.

4- Assistant Professor, Department of Water Science Engineering, Ahvaz Branch, Islamic Azad University, Ahvaz, Iran.

* mo_he3197@yahoo.com

Received: 24 February 2023, Accepted: 19 May 2023  J. Hydraul. Homepage: www.jhyd.iha.ir

Abstract

In the present study, a three-dimensional hydraulic flow simulation was carried out on Labyrinth weirs using Flow3D software and the modeling results were compared with the experimental results to study the discharge coefficient of trapezoidal arced labyrinth weirs. Moreover, these models were tested under laboratory conditions in a rectangular flume with a length of 12m, a width of 0.6m, and a height of 0.6m in clear water conditions. The results indicated that the numerical solution data showed adequate conformity with the experimental model data. In general, the discharge coefficients in the results of the numerical solution were lower than the experimental model. The difference between the discharge coefficients in the numerical solution and the experimental model increased with an increase in the arc radius. As a result, with the $R/w_1=5$ and $R/w_1=15$ radius ratios, the discharge coefficients of the numerical solution were approximately 1.2% and 18.9% lower than the experimental model, respectively.

Keywords: Numerical solution, Flow3D, Discharge Coefficient, Trapezoidal Arced Labyrinth weir.



© 2024 Iranian Hydraulic Association, Tehran, Iran.
This is an open access article distributed under the terms and conditions of the Creative Commons Attribution 4.0 International (CC BY 4.0 license) (<http://creativecommons.org/licenses/by/4.0/>)

1. Introduction

One of the pitfalls of the existing conventional linear weirs is their low discharge capacity due to the limited width of these weirs. The use of labyrinth weirs is considered an efficient and cost-effective solution for increasing the flow rate. These weirs provide a higher discharge capacity for the same hydraulic head than direct weirs due to the increase in the crest length in a given width. The flow running over the weirs within the peak flood hours has to flow within a short period of time. Therefore, it seems necessary to build a weir structure with a high discharge coefficient. Labyrinth weirs are used for this purpose because the amount of flow running through them is larger than linear weirs (Falvey 2003).

Labyrinth weirs are used as cost-effective technical solutions for controlling flow in different conditions such as in dam weirs. Labyrinth weirs may also be used to control discharge capacity, reduce channel water level slope, distribute water between irrigation channels, etc. (Neveen Sad and Fattouh Ehab 2017). The plans of labyrinth weirs are classified into three categories, namely the triangular, trapezoidal and rectangular plans. Most weirs are built with rectangular, trapezoidal, or isosceles plans to increase their performance and facilitate their construction (Crookston 2010). The discharge coefficient in these weirs is determined by various factors such as the weir water level, the walls angle, and the crest thickness and shape (Ghare et al. 2008). The trapezoidal arced labyrinth weir is a cost-effective solution for increasing the efficiency of dams with numerous limitations (such as the limited space and high flood discharge rate) (Ghodsian et al. 2001). Except for the studies conducted by other researchers (Coorkston and Tullis 2012a; Coorkston and Tullis 2012b; Christensen 2012), the other studies have been only conducted on labyrinth weirs with linear cycles or arched noses.

Figure (1) presents the three-dimensional view of the trapezoidal arced labyrinth weir was used in this study.

Bijankhan et al., (2017) proposed a relation for triangular labyrinth weirs under free and submerged flow conditions. They used Buckingham's dimensional analysis approach to determine the relation for the triangular labyrinth weir capacity. In the end, the

discharge coefficient relation was validated using the step-by-step method.

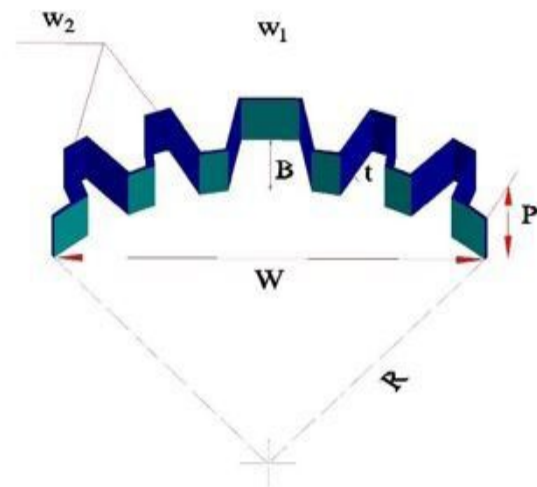


Fig. 1 The trapezoidal arced labyrinth weir with different middle cycles and its parameters (present study)

Bijankhan et al. (2017) carried out research to find the relations and equations for obtaining the weir curves using the Buckingham method. They reviewed the rectangular weir as a commonly used weir with a hydraulic structure and explained its key determining parameters. Afterward, they studied the flow conditions for other types of weirs and finally proposed the discharge capacity relations and tested their application scope. They stated that the extracted relations can be used by the designers of the drainage irrigation networks in the design of weirs.

Emami et al. (2018) carried out a numerical study on the effect of the geometric parameters of labyrinth weirs on their discharge coefficient. A comparison of the results showed that in all cases with different nose angles, the discharge coefficient values were within the satisfactory range for a relatively effective hydraulic head of <0.3 . For a relatively effective hydraulic head higher than 0.3, the discharge coefficient decreased due to the collision of the nappe. Moreover, with an increase in the weir height, the discharge coefficient increased, and thus the labyrinth weir outperformed the linear weir. Azimi et al. (2018) studied flow hydraulics on rectangular labyrinth weirs. According to the results of their experiments, the rectangular labyrinth weir is more sensitive than the sharp linear crested weir in the submerged flow conditions.

Monjezi (2018) carried out an experimental analysis of the flow discharge coefficient in arced labyrinth weirs with triangular plans. The results of their experiments revealed that an increase in the effective length of the weir as a result of its arced plan improves the efficiency of linear arced weirs and labyrinth arced weirs by 21% and 57%, respectively.

Norouzi et al (2019) studied the discharge coefficient (Cd) of a trapezoidal labyrinth weir by using an artificial neural network and vector machines. They found that the MLP model is more acceptable and closer to experimental results.

Gharibvand et al. (2018) studied the flow hydraulics and compared the discharge capacity of trapezoidal labyrinth weirs (two cycles) and piano key weirs (two cycles) through the three-dimensional simulation of the flow field in Flow3D. They also compared the results with the experimental results. The results showed that the numerical modeling data was in line with the experimental model data. According to the results, the piano key weirs had higher discharge coefficients than the labyrinth weirs. Moreover, in the piano key weirs, the discharge coefficient increased by approximately 26 percent with a 50 percent increase in the weir height (P) from 5cm to 7.5cm. In the labyrinth weirs, with a 50 percent increase in the weir height (P) from 5cm to 7.5cm, the discharge coefficient increased by approximately 24 percent.

Ghaderi et al. (2020) studied energy dissipation and hydraulics flow on triangular trapezoidal labyrinth weir (TTLW). They found that the energy dissipation of TTLWs is higher than that of the vertical drop.

Ghaderi et al. (2020) analyzed the hydraulic features of the modified labyrinth weirs numerically. According to the results, modifying the geometry of labyrinth weirs in low sections HT/P ($HT/P < 0.2$) results in an increased discharge coefficient.

Sangsefidi and Ghodsian (2019) conducted an experimental analysis of the effects of headwalls on the performance of arced labyrinth weirs. They studied the effects of the hydraulic head to weir height ratio (H_0/P), the weir side wall angle (α), and the curvature angle (Θ) on the discharge coefficient and efficiency of arced labyrinth weirs while they also analyzed the effects of the angle between the headwalls (Θ'). The results of their research

showed that the arced plan of the labyrinth weir can improve its efficiency.

Crookston et al. (2012) studied the hydraulic performance of trapezoidal labyrinth weirs for high hydraulic head ratios. They performed their physical model experiments on a rectangular flume and prepared the numerical solution using Flow-3D software to compare the results of both the physical and numerical approaches. Their results revealed that Flow-3D software can effectively predict the relation between the discharge coefficient and the trapezoidal labyrinth weir hydraulic head (including a hydraulic head in the weir upstream section in relation to its crest), which is obtained from the experiments conducted on the physical model. Moreover, the hydraulic design curves developed by Crookston (2010) are acceptable for hydraulic head ratios up to 2 or higher.

Crookston et al. (2013) proposed a method for the hydraulic design and analysis of labyrinth weirs based on the experimental results of the physical model. They also proposed the discharge coefficient for labyrinth weirs with quadrant-shaped and semicircular crests and 6 to 35 degrees side angles. In this research, they investigated the nappe behavior, which affects the flow performance, and proposed specific hydraulic design considerations for the nappe characteristics.

Tullis et al. (2018) studied the effect of the scale on labyrinth weirs. They used models with a height of 7.6 cm and 9.14 cm to assess the charging capacity. They realized that the criterion for avoiding the effects of the scale size is negligible depending on the model size and the error rate.

The present study is an attempt to carry out the numerical modeling of the discharge coefficient of a trapezoidal arced labyrinth weir with a middle cycle and different arc radii through a three-dimensional simulation in Flow 3D software and compare its results with the experimental data.

2. Materials and Methods

2.1. Dimensional Analysis

Dimensional analysis is among the basic methods for experimental research, which serves to determine the dimensionless ratios. In the first step of this method, the variables affecting the discharge of labyrinth weirs are identified and then the dimensionless

parameters are determined based on Buckingham's theory, π . After determining the dimensionless parameters, their effect on the discharge of the weirs can be studied to obtain satisfactorily rational results.

2.2. Dimensional Analysis of Trapezoidal Labyrinth Weirs

The general equation for labyrinth weirs, i.e. equation (1), was developed by Lux and Hinchliffe (1985). In this equation, (Q) represents the weir discharge capacity, (L) shows the total length of the weir crest, (g) is the gravitational acceleration, (Hd) is the total hydraulic head, and (Cd) is the dimensionless discharge coefficient, which is determined through experiments.

$$Q = \frac{2}{3} \sqrt{2gC_d} L H_d^{1.5} \quad (1)$$

The parameters affecting the discharge coefficient in arced labyrinth weirs can be expressed via Eq. (2):

$$C_d = f(Q, R, L, B, S, w_1, w_2, W, t, P, D, N, H_d, \lambda, g, \mu, \rho, \sigma) \quad (2)$$

where (Q) is the flow rate, (R) is the radius of the weir arc, (L) is the weir length, (B) shows the length of the weir cycle in the flow direction, (S) is the slope, (w1) is the nose width of the middle cycles, (w2) is the nose width of the side cycles, (W) stands for channel width, (t) shows the weir walls thickness, (P) represents the upstream weir height, (D) is the downstream weir height, (N) shows the number of cycles, (Hd) is the hydraulic head of the entire flow on the weir upstream, (λ) is the crest section shape factor, (g) is the gravitational acceleration, and σ , ρ , and μ respectively denote dynamic viscosity, density and surface tension of water. For the dimensional analysis, parameters P, ρ and Q are considered the repetitive variables and the dimensionless parameters are obtained through Eq. (3):

$$C_d = f(B/P, t/P, D/P, W/P, N, \lambda, H_d/P, S, g, P_5/Q_2, \mu P/\rho Q, w_1/P, R/w_1, w_2/P, \rho P_8/q_2 \sigma) \quad (3)$$

After omitting the channel slope (S), the width of a cycle (W), the weir wall thickness (t), the

upstream weir height (P), the downstream weir height (D), the number of cycles (N), the channel slope (S), the middle cycle nose width (w1), the side cycles nose width (w2), the weir cycle length in the flow direction (B), the crest section shape factor (λ), and the gravitational acceleration (g) that is constant are overlooked with the dimensional analysis technique. Moreover, the effect of the Reynolds dimensionless number ($\mu P/\rho Q$) and Weber number ($\rho P_8/Q_2 \sigma$) is overlooked in all experiments of the present study because of the turbulent flow and the inadequate flow depth. It is worth stating that the effect of the gravitational acceleration (gP_5/Q_2), which represents the Froude number, is included in the dimensionless parameter (Hd/P). By combining the weir radius ratio (R/P) with the middle cycle width ratio (w1/P), the dimensionless and variable parameter (R/w1) is obtained. Therefore, the relation for the dimensionless parameters affecting the discharge coefficient of trapezoidal labyrinth weirs in this study is written as follows (4).

$$C_d = f(H_d/P, R/w_1) \quad (4)$$

2.3. The Experimental Model

Due to the need for adequate laboratory space and a standard and equipped laboratory flume for performing the experiments in this study with acceptable quality, the researchers used the space and facilities of the hydraulic laboratory of the Water and Electricity Organization of Khuzestan Province, Iran. As regards the geometric specifications of the laboratory flume used in this study, it has a rectangular cross-section, a length of 6 meters, a width of 0.6 meters, and a height of 0.6 meters. The flume walls are transparent and made of Plexiglas, and the water surface profile and the flow conditions are visible. The flow running over the weir is also free flow. To increase the accuracy of the results of the experiments, the flume is examined prior to the experiments to ensure it is sealed and there is no crack in its different parts. The flume bed is a fixed, flat and horizontal bed. The water flow is initially pumped from the ground tank to an elevated tank, and then enters the beginning of the flume through the pipeline. Here, the water flow is controlled by a valve, and then the flow enters the channel slowly with a low discharge capacity. The flow slowly runs over the weir,

which is placed on the flume bed. With the variation of the discharge capacity, the hydraulic condition of the weir is studied and recorded. Finally, the water flow passes through the weir and enters the pumping tank via the downstream channel and returns to the open cycle. The specifications of the different flume sections and the laboratory equipment used in this research are presented in Figure 2. To relieve the weir upstream flow and reduce the water surface fluctuations, a metal lattice and a polystyrene component are used in the flume inlet.

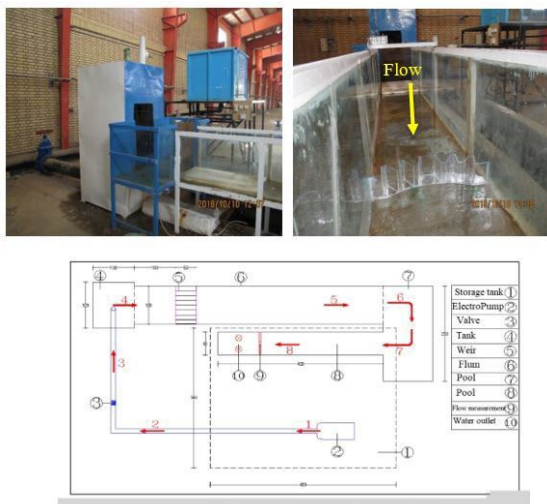


Fig. 2 The overall view of the laboratory flume and equipment used in the present study

To compare the results of the numerical solution and experimental model, the best weir models were selected and simulated from all the tested models with regard to the discharge capacity and discharge coefficient using a certain

geometrical criterion for comparing and improving the selection results. To this end, a total of 36 experiments were conducted using 3 physical models of trapezoidal arced labyrinth weirs with different middle cycles and constant parameters such as a total cycle width (W) of 600mm, a thickness (t) of 5mm, a cycle number (N) of 5, a side cycle nose width to the middle cycle nose width ratio of 0.30 (w_2/w_1), and a cycle length to the middle nose width (B/w_1) of 1 in three different arc states. Each experiment was repeated three times and when the numerical results of two experiments were similar, those results were recorded. Figure 3 shows the three models of the study weirs in this study, which were made of Plexiglas.



Fig. 3 A view of the trapezoidal arced labyrinth weirs

It is worth stating that at the time of placing the weirs the alignment of their crests was checked based on the builder's level. In addition, the perpendicularity of the weir wall to the flume bed was controlled using a set square both in the installation phase and after the placement of water behind the weir. The geometric and hydraulic specifications of the arced labyrinth weirs used in this research are listed in Table 1.

Table 1. The geometric and hydraulic specifications of arced labyrinth weirs

Model	W (m)	R (m)	L (m)	t (m)	N	w_2/w_1	B/w_1	Number of Test	$Q(m^3/s)$
1	0.60	0.45	1.36	0.005	5	0.30	1	12	0.005-0.05
2	0.60	0.90	1.33	0.005	5	0.30	1	12	0.005-0.05
3	0.60	1.35	1.31	0.005	5	0.30	1	12	0.005-0.05

In the tables above, W is the flume cycle width, R is the weir arc radius, L is the effective length of the weir, t is the weir thickness, B is the weir cycle length, w_2 is the width of the side cycles nose, w_1 is the width of the nose of the middle cycles, and N is the number of cycles in the weir.

2.4. Numerical Solution

Flow3D software is a suitable model with a wide range of applications to the analysis of complex fluid problems, including unsteady three-dimensional flows with a free surface and a complex geometry. In this software, the finite volume method is used for regular rectangular

meshing. When using the finite volume method in a regular mesh, the discrete equations are similar to the discrete equations in the finite difference method. Moreover, two-equation models are mainly used to model turbulence in hydraulic problems. In this research, the KW model is used to close the Reynolds time-averaged equations. Flow3D software is used for the numerical part to numerically solve the governing non-steady equations with the finite volume method. In this software, the Fractional Area-Volume Obstacle Representation or FAVOR algorithm is used to define the geometry in the finite volume method. In this algorithm, the obstacles in the field in the calculated cells are considered partial values varying between 0 and 1. If the entire cell is filled with the obstacle, the fractional area or volume value equals 1. The free flow surface is determined by the volume of fluid (VOF) algorithm. The velocity and pressure terms are also coupled implicitly using the past values of pressure and velocity in the continuity and momentum equations. In this software, the resulting quasi-implicit equations are solved repeatedly using attenuation techniques. In this paper, the generalized minimal residual (GMRES) method serves as an implicit pressure solver to increase the accuracy of the results. The Flow3D numerical solution creates a three-dimensional structured mesh that is composed of cubic-rectangular cells for the field. Therefore, first, a three-dimensional model in line with the specifications of the experimental models was created using AutoCAD software, and then the resulting geometry was introduced to Flow3D software using the VOF and FAVOR tools to determine the boundaries and the calculated mesh. After entering the geometric data into the software and determining the boundaries of the primary and secondary channels, the area was meshed using the VOF and FAVOR methods. Thereafter, the optimal mesh dimensions were selected based on the required accuracy and time allocated to the calculations, and the field mesh was designed to create orthogonal mesh lines. After creating the geometry of the weirs and transferring it to Flow3D, meshing was performed and the boundary conditions along with the input conditions were determined. In this research, a total of 120 thousand cells on average were selected for three single-block meshes with different cell dimensions in X, Y and Z to mesh the models and perform the

calculations. After generating the calculated mesh and determining the boundary conditions and the initial conditions, water flow was simulated. A mesh type with different sizes was selected for the simulation of the weirs. As seen in Figure 4, in type 1 meshing, the boundary conditions for the flume walls and bed, the flume inlet, the flume outlet, and the flow surface that was exposed to air the boundary conditions were the wall boundary conditions, the inflow discharge capacity boundary condition, the outflow boundary condition, and the specified pressure boundary condition, respectively.

3. Results and Discussion

The comparison of the experimental results with the results of the numerical solution for the discharge coefficient of trapezoidal arced labyrinth weirs with different middle cycles and different arc ratios in Flow-3D software is presented in the following diagrams.

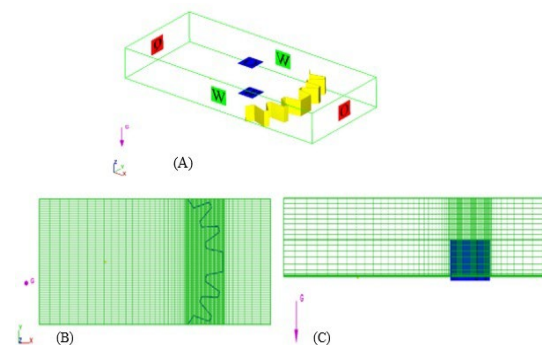


Fig. 4 The boundary conditions created for the trapezoidal arced labyrinth weir used in this study: A- three-dimensional view, B-the above view, and C-the side view

3.1. Analyzing the discharge coefficient of trapezoidal arced labyrinth weirs resulting from the numerical and experimental models with 5, 10, and 15 arc radii ($R/w_1 = 5, 10, 15$)

As seen in Figures (5), (6) and (7), the discharge coefficient decreased with an increase in the hydraulic head. In other words, the results of the numerical model show lower discharge coefficient values than the experimental model. In these figures, the trapezoidal labyrinth weir has a hydraulic head ratio of 0.1 to 0.7 in the adhesion and complete aeration phase and from 0.7 to 1 in the partial aeration and suffocation stage. Moreover, the arc radius ratio of 15 has the highest discharge coefficient values as

compared to the 10 and 5 ratios. In other words, with an increase in the arc radius ratio, the hydraulic efficiency of the weir increases along with its hydraulic efficiency. As seen in Figures (6) and (7), with an increase in the hydraulic head, the difference between the discharge coefficients in the numerical and experimental models decreased. Moreover, according to these diagrams, with an increase in the arc radius, the difference between the discharge

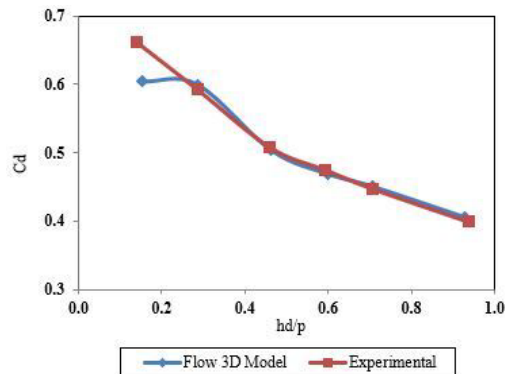


Fig. 5 Comparing the results of the numerical solution and experimental models for the arc radius ratio of 5 ($R/w_1=5$)

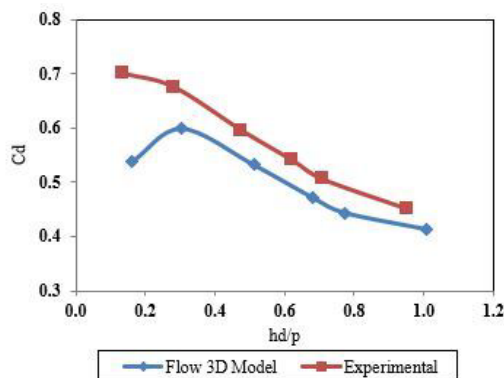


Fig. 6 Comparing the results of the numerical solution and experimental models for the arc radius ratio of 10 ($R/w_1=10$)

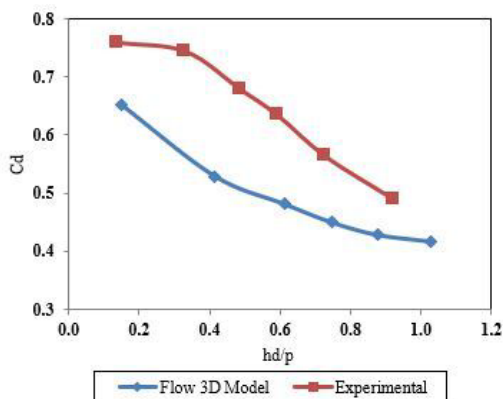


Fig. 7 Comparing the results of the numerical solution and experimental models for the arc radius ratio of 15 ($R/w_1=15$)

coefficients in the numerical and experimental models increased, which could be attributed to an error in the numerical solution in detecting the small variations in the arc radius. In other words, in the numerical model, the discharge coefficient did not differ significantly from the arc radius variations, whereas in the experimental model, the effect of the arc radius on the discharge coefficient was more significant.

Figure (8) presents the numerical simulation environment in Flow3D. In Table 2, the numerical and experimental values of the discharge coefficient of the trapezoidal labyrinth weir are presented.

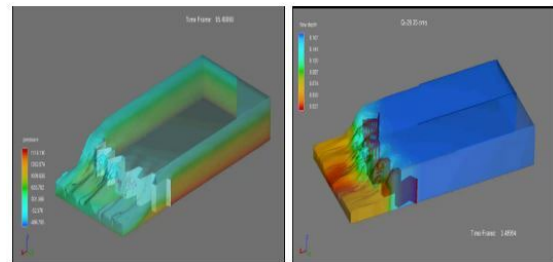


Fig. 8 Pattern of flow running over the trapezoidal labyrinth weir

Table 2. Comparing the results of the numerical solution and experimental modeling for the C_d value with the percent error

R/w_1	Result of C_d		h_d/P	percent error
	Experimental	Flow3d model		
$R/w_1=5$	0.64	0.61	0.2	4.7
	0.52	0.64	0.4	0
	0.46	0.52	0.6	0
	0.43	0.46	0.8	0
	0.41	0.43	0.9	0
$R/w_1=10$	0.68	0.55	0.2	19.1
	0.63	0.58	0.4	7.9
	0.54	0.50	0.6	7.4
	0.48	0.44	0.8	8.3
	0.46	0.42	0.9	8.7
$R/w_1=15$	0.76	0.64	0.2	15.8
	0.71	0.53	0.4	25.3
	0.63	0.49	0.6	22.2
	0.53	0.45	0.8	15.1
	0.50	0.42	0.9	16

4. Conclusion

A comparison of labyrinth weir discharge coefficients resulting from the numerical and experimental models revealed that the discharge coefficients of the experimental

values are higher than the numerical modeling results. Besides, the labyrinth weir properly completes the four hydraulic stages in the experimental and numerical conditions, reflecting the proper hydraulic performance of the weir. When the weir is in the full aeration state, the weir is in the maximum hydraulic efficiency state. It is worth stating that when the weir is in the partial aeration condition, its hydraulic efficiency starts to decline. Finally, if it reaches the suffocation stage, the weir loses its hydraulic efficiency, the energy is maximized, the entire length of the weir crest is fully submerged, and thus the weir functions as an obstacle in the flow path. The energy loss is maximized when the hydraulic head is maximized. As a result, the nappes collide in the weir outflow keys, resulting in a drastic energy loss. From the quantitative viewpoint, in the weir with a radius ratio of $R/w_1=5$, the numerical and experimental results satisfactorily overlap, and for $h_d/p>0.2$ in the two diagrams, they are fully in line. In the weir with the $R/w_1=10$ radius ratio, the numerical solution outflow discharge coefficient is 10.2 percent smaller than the experimental results on average. Besides, with the $R/w_1=15$ radius ratio in the results of the numerical model, the discharge coefficients are approximately 18.9 percent lower than the experimental model. In general, with an increase in the weir arc radius, the difference between the flow coefficients in the numerical solution and the experimental results increases.

5. Notation

Q	Discharge
R	Radius of the weir arc
L	Weir length
B	Shows the length of the weir cycle in the flow direction
S	Slope
P	Represents the upstream weir height
W	Stands for channel width
w_1	Nose width of the middle cycles
w_2	Nose width of the side cycles
t	Weir walls thickness
D	Downstream weir height
N	Number of cycles
H_d	Hydraulic head (the entire flow on the weir upstream)
λ	Crest section shape factor
g	Gravitational acceleration
μ	Dynamic viscosity
ρ	Density
σ	Surface tension of water

C_d	Discharge coefficient
w_2/w_1	Side cycle nose width to the middle cycle nose width
B/w_1	Cycle length to the middle nose width
R/w_1	Arc radius ratio
H_d/P	Hydraulic head to weir height ratio

6. Acknowledgments

The authors would like to thank the Water and Power Authority of Khuzestan, Iran for their support in providing the required laboratory equipment.

7. References

- Ghaderi, A., Daneshfaraz, R., Dasineh, M. & Di Francesco, S. (2020). Energy Dissipation and Hydraulics of Flow over Trapezoidal–Triangular Labyrinth Weirs. *Water*, 12(7), 1992, <https://doi.org/10.3390/w12071992>.
- Ghaderi, A., Daneshfaraz, R., Abbasi, S. & Abraham, J. (2020). Numerical analysis of the hydraulic characteristics of modified labyrinth weirs. *International Journal of Energy and Water Resources*, 4, 425–436.
- Azimi, A. & Seyed Hakim, S. (2018). Hydraulics of flow over rectangular labyrinth weirs. *Irrig Sci*, 37(12), 183–193.
- Bijankhan, M. & Ferro, V. (2017). Dimensional analysis and stage-discharge relationship for weirs: A review. *J. Agri Eng.*, 48(1), 1–11.
- Bijankhan, M. & Kouchakzadeh, S. (2017). Unified discharge coefficient formula for free and submerged triangular labyrinth weirs. *Flow Meas Instrum*, 57, 46–56.
- Christensen, N.A. (2012). Flow Characteristics of Arced Labyrinth Weirs. MSc thesis, Utah State University, Logan, Utah.
- Crookston, B.M. & Tullis, B.P. (2013). Labyrinth Weirs: Nappe Interference and Local Submergence. *J Irrig Drain Eng.*, 138(8), 757–765.
- Crookston, B.M. & Tullis, B.P. (2012a). Arced labyrinth weirs. *J Hydraul Eng*, 138(6), 555–562.
- Crookston, B.M. & Tullis, B.P. (2012b). Discharge efficiency of reservoir-application-specific labyrinth weirs. *J Irrig Drain Eng*, 138(6), 773–776.
- Crookston, B.M. (2010) Labyrinth weirs. PhD thesis, Utah State University, Logan, Utah.

- Emami, S., Arvanaghi, H. & Parsa, J. (2018). Numerical Investigation of Geometric Parameters Effect of the Labyrinth Weir on the Discharge Coefficient. *J Rehabil Civ Eng*, 6(1), 01-09.
- Falvey, H.T. (2003). Hydraulic Design of Labyrinth Weirs. USA, ASCE press.
- Ghare, A.D., Mhaisalkar, V.A. & Porey, P.D. (2008). An Approach to Optimal Design of Trapezoidal Labyrinth Weirs. *World. Appl Sci J*, 3(6), 934-938.
- Gharibvand, R., Heidarnejad, M., Kashkoli, H.A., Hasounizadeh, H. & Kamanbedast, A.A. (2018). Numerical analysis of flow hydraulic in trapezoidal labyrinths and piano key weirs. *Flow Meas Instrum*, 64, 64-70.
- Ghodsian, D., Amanian, N. & Marashi, S.A. (2001). Discharge Coefficient of Semicircular Labyrinth Weirs. *Amirkabir J Civil Eng Tehran*, 13, 76-83. (In Persian)
- Lux, F. & Hinchliff, D.L. (1985). Design and construction of labyrinth spillways. In: Proceedings of 15th ICOLD Congress, Q59(R15), 249-274; Lausanne, Switzerland.
- Monjezi, R., Heidarnejad, M., Masjedi, A.R., Purmohammadi, M.H. & Kamanbedas, A.A. (2018). Laboratory Investigation of the Discharge Coefficient of Flow in Arced Labyrinth Weirs with Triangular Plans. *Flow. Meas. Instrum*, 64, 64-70.
- Neveen, Y.S. & Fattouh Ehab, M. (2017). Hydraulic characteristics of flow over weirs with circular openings. *Ain Shams Eng J.*, 8, 515-522.
- Norouzi, R., Daneshfaraz, R. & Ghaderi, A. (2019). Investigation of discharge coefficient of trapezoidal labyrinth weirs using artificial neural networks and support vector machines. *Journal of Applied Water Science*, 148(9), 1-10.
- Sangsefidi, Y. & Ghodsian, M. (2019). Investigation of Effects of Entrance Channel Walls on the Hydraulic Performance of Arced Labyrinth Weirs. *Modares Civil Eng J.*, 19(1), 181-193. (In Persian)
- Tullis, B.P. (2018). Size-Scale Effects of Labyrinth Weir Hydraulics. In: Proceedings of 7th IAHR International Symposium on Hydraulic Structures, 15-18.